

1 Revision 2

2

3 **Lead–tellurium oxysalts from Otto Mountain near Baker, California: VIII. Fuettererite,**
4 **$\text{Pb}_3\text{Cu}^{2+}_6\text{Te}^{6+}\text{O}_6(\text{OH})_7\text{Cl}_5$, a new mineral with double spangolite–type sheets.**

5

6 Anthony R. Kampf^{1,*}, Stuart J. Mills², Robert M. Housley³, and Joseph Marty⁴

7

8 ¹Mineral Sciences Department, Natural History Museum of Los Angeles County,
9 900 Exposition Blvd., Los Angeles, CA 90007, U.S.A.

10 ²Geosciences, Museum Victoria, GPO Box 666, Melbourne 3001, Victoria, Australia

11 ³Division of Geological and Planetary Sciences, California Institute of Technology, Pasadena,
12 CA 91125, U.S.A.

13 ⁴5199 E. Silver Oak Road, Salt Lake City, UT 84108, U.S.A.

14

15 *e-mail: akampf@nhm.org

16

17 **ABSTRACT**

18 Fuettererite, $\text{Pb}_3\text{Cu}^{2+}_6\text{Te}^{6+}\text{O}_6(\text{OH})_7\text{Cl}_5$, is a new tellurate from Otto Mountain near Baker,
19 California, named for Otto Fuetterer who is largely responsible for the development of the
20 mining claims on Otto Mountain. The new mineral is known from only two specimens, one from
21 the NE2 vein and the other from the Bird Nest drift. Fuettererite occurs in vugs in quartz, on the
22 first specimen associated with Br-rich chlorargyrite, iodargyrite, and telluroperite and on the
23 second specimen associated with anglesite, anatacamite, atacamite, chalcopyrite, galena, goethite,
24 hematite, muscovite, phosphohedyphane, timroseite, and wulfenite. It is interpreted as having

25 formed from the partial oxidation of primary sulfides and tellurides during or following
26 brecciation of quartz veins. Fuettererite is hexagonal, space group $R\bar{3}$, $a = 8.4035(12)$, $c =$
27 $44.681(4)$ Å, $V = 2732.6(6)$ Å³ and $Z = 6$. Crystals are tabular to short prismatic, exhibit the
28 forms $\{100\}$, $\{101\}$, and $\{001\}$ and reach a maximum dimension of 50 µm. The color is bluish
29 green, the streak is pale bluish-green, and the luster is adamantine. The Mohs hardness is
30 estimated at between 2 and 3. The new mineral is brittle with irregular fracture and one perfect
31 cleavage on $\{001\}$. The calculated density based on the empirical formula is 5.528 g/cm³.
32 Fuettererite is uniaxial (-), with calculated indices of refraction of $\omega = 2.04$ and $\varepsilon = 1.97$, and is
33 dichroic bluish-green, $E < O$. Electron microprobe analysis provided: PbO 41.45, CuO 30.35,
34 Al₂O₃ 0.23, TeO₃ 12.80, Cl 12.08, H₂O 3.55 (structure), O=Cl -2.73, total 97.73 wt%. The
35 empirical formula (based on 18 O + Cl atoms *pfu*) is:
36 $\text{Pb}_{2.88}\text{Cu}^{2+}_{5.92}\text{Al}_{0.07}\text{Te}^{6+}_{1.13}\text{O}_{6.59}(\text{OH})_{6.12}\text{Cl}_{5.29}$. The ten strongest powder X-ray diffraction lines are
37 [d_{obs} in Å (hkl) I]: 6.106 (104) 44, 3.733 (0·0·12) 100, 2.749 (12-1) 53, 2.6686 (12-4) 49, 2.5289
38 (12-7) 41, 2.2772 (1·2·11) 38, 1.9637 (315, 1·2·-16) 87, 1.8999 (multiple) 48, 1.5976 (multiple)
39 40, and 1.5843 (410, 1·2·23, 143) 44. The crystal structure of fuettererite ($R_1 = 0.031$ for 971
40 reflections with $F_o > 4\sigma F$) contains edge-sharing sheets of CuO₅Cl and TeO₆ octahedra. These
41 sheets are virtually identical to that in the structure of spangolite, but in fuettererite they are
42 linked together to form a double sheet. The double octahedral sheets alternate with thick double
43 layers of PbO₂Cl₆ polyhedra. The CuO₅Cl octahedra exhibit pronounced Jahn-Teller distortions
44 and the PbO₂Cl₆ polyhedron has a lopsided distribution of bond lengths attributable to the
45 localization of the Pb²⁺ 6s² lone-pair electrons.

46

47 Keywords: Fuettererite; new mineral; tellurate; crystal structure; spangolite; $\text{Pb}^{2+} 6s^2$ lone-pair;
48 Otto Mountain, California.

49

50

INTRODUCTION

51 During the course of continuing investigations of the remarkable secondary mineral
52 assemblage at Otto Mountain, near Baker, California (Housley et al. 2011), we have thus far
53 described eight new Pb–Te oxysalts: ottoite, housleyite, thorneite, markcooperite, timroseite,
54 paratimroseite, telluroperite, and chromscheffelinite (see Table 1), and have reported the structure
55 determination of munakataite (Kampf et al. 2010g). In this contribution, we describe fuettererite
56 and in the accompanying paper we describe agaite (Kampf et al. 2012b), the ninth and tenth new
57 Pb–Te oxysalt minerals from this deposit.

58 The new mineral is named fuettererite in honor of Otto Fuetterer (born *ca.* 1880; died *ca.*
59 1970), who is largely responsible for the development of the mining claims on Otto Mountain. In
60 1940, Fuetterer, a naturalized American citizen born in Germany and then about 60 years old,
61 filed six claims on the hill named Good Hope 1–6. The following year a friend of his, A. G.
62 Andrews (AGA), filed 18 adjacent claims named Aga 1–18; in 1942 Andrews added two more,
63 Aga 19 and 20. They held these claims together until sometime after 1950 when Fuetterer
64 became sole owner of all 26 claims. According to Lois Clark, Baker resident and longtime friend
65 of Fuetterer, he was a well-educated man and had an appreciation and understanding of the
66 sciences. He continued to live on and work the claims until near the time of his death around
67 1970. During the time he lived on the mountain, originally named “Hopeless Hill”, people in
68 Baker came to call it Otto Mountain and that name, and the name Aga mine stuck when the U. S.
69 Geological Survey produced their latest series of maps. It is worth noting that the new mineral
70 ottoite was named for the locality, rather than for Otto Fuetterer.

71 The new mineral and name has been approved by the Commission on New Minerals,
72 Nomenclature and Classification of the International Mineralogical Association (IMA 2011–
73 111). One holotype and one cotype specimen are deposited in the Natural History Museum of
74 Los Angeles County, catalogue number 63588 and 64589, respectively.

75

76

OCCURRENCE

77 The holotype specimen of fuettererite was found at a small prospect in a quartz vein
78 referred to as the NE2 vein (35.27776°N, 116.09331°W, elevation 1090 feet) on the northeast
79 flank of Otto Mountain, about 0.4 miles north of the Aga mine. The cotype specimen is from the
80 Bird Nest drift (35.27677°N, 116.09927°W) on the southwest flank of Otto Mountain, 0.4 miles
81 northwest of the Aga mine.

82 Fuettererite is very rare. It has been found on only two specimens. The holotype specimen
83 was found by two of the authors (RMH and JM). On this specimen, about 10 crystals of the
84 mineral occur scattered in a vug in quartz closely associated with Br-rich chlorargyrite,
85 iodargyrite, and telluroperite. The cotype specimen was found by Jerry A. Baird of Lake Havasu
86 City, Arizona. On this specimen, tiny fuettererite crystals occur intergrown with paratacamite in
87 vugs in quartz. Other minerals that occur on this specimen include anglesite, anatacamite,
88 atacamite, chalcopyrite, galena, goethite, hematite, muscovite, phosphohedyphane, timroseite,
89 and wulfenite. Other species identified in the mineral assemblages at Otto Mountain include
90 acanthite, agaite, boleite, brochantite, burckhardtite, calcite, caledonite, celestine, cerussite,
91 chromschiefelinite, chrysocolla, devilline, diaboite, eztlite, fluorite, fornacite, gold, hessite,
92 housleyite, jarosite, khinite, kuranakhite, linarite, malachite, markcooperite, mimetite,

93 mottramite, munakataite, murdochite, ottoite, paratimroseite, perite, plumbojarosite, pyrite,
94 thorneite, vanadinite, and vauquelinite.

95 Fuettererite occurs as a secondary oxidation zone mineral and is presumed to have formed
96 by oxidation of tellurides, chalcopyrite and galena. Additional background on the occurrence is
97 provided in Kampf et al. (2010a) and Housley et al. (2011).

98

99

PHYSICAL AND OPTICAL PROPERTIES

100 On the holotype specimen, the mineral occurs as thick tabular to short prismatic crystals
101 up to about 50 μm in maximum dimension and exhibiting the forms $\{100\}$ and $\{001\}$. On the
102 cotype specimen, fuettererite occurs as tablets up to about 10 μm in diameter and 2 μm thick and
103 exhibiting the forms $\{101\}$ and $\{001\}$ (Figs. 1 and 2). No twinning was observed optically under
104 crossed polars or based upon single-crystal X-ray diffraction. The color is bluish green, the streak
105 is pale bluish green, and the luster is adamantine. The Mohs hardness could not be measured, but
106 is estimated to be between 2 and 3. The new mineral is brittle with irregular fracture and one
107 perfect cleavage on $\{001\}$. The density could not be measured because it is greater than those of
108 available high-density liquids and there is insufficient material for physical measurement. The
109 calculated density based on the empirical formula is 5.528 g/cm^3 and that based on the ideal
110 formula is 5.552 g/cm^3 . Fuettererite is readily soluble in cold dilute HCl.

111 Crystals of fuettererite are uniaxial (–) with the indices of refraction $\omega = 2.04$ and $\varepsilon =$
112 1.97, calculated from the retardation = 0.07 (measured with a Berek compensator) and $n_{\text{av}} =$
113 2.015 (based upon the Gladstone–Dale relationship). The mineral is dichroic bluish green, $E < O$.

114

115

CHEMICAL COMPOSITION

116 Quantitative chemical analyses of fuettererite were performed using a JEOL8200 electron
117 microprobe (WDS mode, 15 kV, 5 nA, 1 μm beam diameter) at the Division of Geological and
118 Planetary Sciences, California Institute of Technology. The standards used were: galena (for Pb),
119 cuprite (for Cu), anorthite (for Al), Sb_2Te_3 (for Te), and sodalite (for Cl). Analytical results are
120 given in Table 2. No other elements were detected in EDS analyses. There was insufficient
121 material for CHN analyses, so H_2O was calculated on the basis of 10 total cations (Pb + Cu + Al
122 + Te), charge balance and 18 total anions (O + Cl) *pfu*, as determined by the crystal structure
123 analysis (see below). Note that fuettererite is prone to electron beam damage, which contributes
124 to the low analytical total. This is a common feature observed in most secondary tellurate species
125 (e.g. Kampf et al. 2010a–e; Kampf et al. 2012a,b; Mills et al. 2009, 2010).

126 The empirical formula (based on 18 O + Cl atoms *pfu*) is:
127 $\text{Pb}_{2.88}\text{Cu}^{2+}_{5.92}\text{Al}_{0.07}\text{Te}^{6+}_{1.13}\text{O}_{6.59}(\text{OH})_{6.12}\text{Cl}_{5.29}$. The simplified formula is $\text{Pb}_3\text{Cu}^{2+}_6\text{Te}^{6+}\text{O}_6(\text{OH})_7\text{Cl}_5$,
128 which requires PbO 43.97, CuO 31.34, TeO_3 11.53, Cl 11.64, H_2O 4.14, O=Cl –2.63, total 100
129 wt%.

130

131 X-RAY CRYSTALLOGRAPHY AND STRUCTURE DETERMINATIONS

132 All powder and single-crystal X-ray diffraction data were obtained on a Rigaku R-Axis Rapid II
133 curved imaging plate microdiffractometer utilizing monochromatized $\text{MoK}\alpha$ radiation. Observed
134 powder *d*-values (with standard deviations) and intensities were derived by profile fitting using
135 JADE 9.3 software. Data (in \AA) are given in Table 3. Unit cell parameters refined from the
136 powder data using JADE 9.3 with whole pattern fitting are: $a = 8.401(5)$, $c = 44.68(3)$ \AA , and $V =$
137 $2731(3)$ \AA^3 . The observed powder data fit well with those calculated from the structure, also

138 using JADE 9.3. The relatively low precision of the cell refined from the powder data is
139 attributable to the use of $\text{MoK}\alpha$ radiation.

140 The Rigaku CrystalClear software package was used for processing of the diffraction
141 data, including the application of an empirical multi-scan absorption correction using ABSCOR
142 (Higashi 2001). The structure was solved by direct methods using SIR2004 (Burla et al. 2005).
143 SHELXL-97 software (Sheldrick 2008) was used for the refinement of the structure. H atom
144 positions were located in difference Fourier maps and were constrained to H–O distances of
145 $0.90(3)$ Å with isotropic displacement parameters ($\times 1.2$) tied to those of the O atoms to which
146 they are associated. Attempts to refine the occupancies of the cation sites indicated all to be very
147 close to fully occupied and did not improve the value of R_1 substantially (0.0304 vs 0.0307);
148 therefore, we report the refinement with all sites fully occupied and consistent with the ideal
149 formula. Details concerning data collection and structure refinement are provided in Table 4.
150 Fractional coordinates and atom displacement parameters are provided in Table 5, selected
151 interatomic distances in Table 6 and bond valences in Table 7.

152

153 DESCRIPTION OF THE STRUCTURE

154 The structure (Fig. 3) contains edge-sharing sheets of CuO_5Cl and TeO_6 octahedra parallel
155 to $\{001\}$. The two independent CuO_5Cl octahedra exhibit pronounced Jahn-Teller distortions
156 with particularly long apical Cu–Cl distances. Each CuO_5Cl octahedron is associated with
157 equivalent octahedra in an edge-sharing trimer lying on a threefold axis, with Cl as the common
158 vertex. The Cl vertex extends significantly out of the plane of the sheet, where it also participates
159 as a shared corner with an equivalent trimer in an adjacent sheet. This linkage, along with
160 hydrogen bonds, serves to create double octahedral sheets (Fig. 4). The double octahedral sheets

161 alternate along *c* with thick double layers of PbO₂Cl₆ polyhedra. The PbO₂Cl₆ polyhedron has a
162 lopsided distribution of bond lengths attributable to the localization of the Pb²⁺ 6s² lone-pair
163 electrons (Fig. 5).

164 The octahedral sheet is virtually identical to that in the structure of spangolite,
165 Cu₆Al(SO₄)(OH)₁₂Cl·3H₂O, except that in spangolite it is composed of CuO₅Cl, CuO₆ and AlO₆
166 octahedra (Figs. 3 and 6). The structures also differ in that spangolite has only single octahedral
167 sheets and the common vertex of each Cu octahedral trimer links to a SO₄ tetrahedron. In the
168 spangolite structure, SO₄ and H₂O groups rather than Pb polyhedra occur between the octahedral
169 sheets and the sheets are linked to one another only via hydrogen bonding (Fig. 4).

170

171

ACKNOWLEDGEMENTS

172 The paper benefited from comments by reviewers Chi Ma and John M. Hughes. Jerry
173 Baird is thanked for providing the cotype specimen of fuettererite. The Caltech EMP analyses
174 were supported by a grant from the Northern California Mineralogical Association. The
175 remainder of this study was funded by the John Jago Trelawney Endowment to the Mineral
176 Sciences Department of the Natural History Museum of Los Angeles County.

177

178

REFERENCES

179 Burla, M.C., Caliendo, R., Camalli, M., Carrozzini, B., Cascarano, G.L., De Caro, L.,
180 Giacobozzo, C., Polidori, G., and Spagna, R. (2005) SIR2004: an improved tool for crystal
181 structure determination and refinement. *Journal of Applied Crystallography*, 38, 381–388.
182 Brese, N.E. and O’Keeffe, M. (1991) Bond-valence parameters for solids. *Acta*
183 *Crystallographica*, B47, 192–197.

- 184 Brown, I.D. and Altermatt, D. (1985) Bond-valence parameters from a systematic analysis of the
185 inorganic crystal structure database. *Acta Crystallographica*, B41, 244–247.
- 186 Hawthorne, F.C., Kimata, M., and Eby, R.K. (1993) The crystal structure of spangolite, a
187 complex copper sulfate sheet mineral. *American Mineralogist*, 78, 649–652.
- 188 Higashi, T. (2001) *ABSCOR*. Rigaku Corporation, Tokyo, Japan.
- 189 Housley, R. M., Kampf, A. R., Mills, S. J., Marty, J., and Thorne, B. (2011) The remarkable
190 occurrence of rare secondary tellurium minerals at Otto Mountain near Baker, California –
191 including seven new species. *Rocks and Minerals*, 86, 132–142.
- 192 Kampf, A. R., Housley, R. M., Mills, S. J., Marty, J. and Thorne, B. (2010a) Lead–tellurium
193 oxysalts from Otto Mountain near Baker, California: I. Ottoite, Pb_2TeO_5 , a new mineral
194 with chains of tellurate octahedra. *American Mineralogist*, 95, 1329–1336.
- 195 Kampf, A. R., Marty, J. and Thorne, B. (2010b) Lead–tellurium oxysalts from Otto Mountain
196 near Baker, California: II. Housleyite, $\text{Pb}_6\text{CuTe}_4\text{TeO}_{18}(\text{OH})_2$, a new mineral with Cu–Te
197 octahedral sheets. *American Mineralogist*, 95, 1337–1342.
- 198 Kampf, A. R., Housley, R. M. and Marty, J. (2010c) Lead–tellurium oxysalts from Otto
199 Mountain near Baker, California: III. Thorneite, $\text{Pb}_6(\text{Te}_2\text{O}_{10})(\text{CO}_3)\text{Cl}_2(\text{H}_2\text{O})$, the first
200 mineral with edge-sharing octahedral dimers. *American Mineralogist*, 95, 1548–1553.
- 201 Kampf, A. R., Mills, S. J., Housley, R. M., Marty, J. and Thorne, B. (2010d) Lead–tellurium
202 oxysalts from Otto Mountain near Baker, California: IV. Markcooperite, $\text{Pb}_2(\text{UO}_2)\text{TeO}_6$,
203 the first natural uranyl tellurate. *American Mineralogist*, 95, 1554–1559.
- 204 Kampf, A. R., Mills, S. J., Housley, R. M., Marty, J. and Thorne, B. (2010e) Lead–tellurium
205 oxysalts from Otto Mountain near Baker, California: V. Timroseite,

- 206 $\text{Pb}_2\text{Cu}^{2+}_5(\text{Te}^{6+}\text{O}_6)_2(\text{OH})_2$, and paratimroseite, $\text{Pb}_2\text{Cu}^{2+}_4(\text{Te}^{6+}\text{O}_6)_2(\text{H}_2\text{O})_2$, new minerals
207 with edge-sharing Cu–Te octahedral chains. *American Mineralogist*, 95, 1560–1568.
- 208 Kampf, A. R., Mills, S. J., Housley, R. M., Marty, J. and Thorne, B. (2010f) Lead–tellurium
209 oxysalts from Otto Mountain near Baker, California: VI. Telluroperite, $\text{Pb}_3\text{Te}^{4+}\text{O}_4\text{Cl}_2$, the
210 Te analogue of perite and nadorite. *American Mineralogist*, 95, 1569–1573.
- 211 Kampf, A. R., Mills, S. J. and Housley, R. M. (2010g) The crystal structure of munakataite,
212 $\text{Pb}_2\text{Cu}_2(\text{Se}^{4+}\text{O}_3)(\text{SO}_4)(\text{OH})_4$, from Otto Mountain, San Bernardino County, California,
213 USA. *Mineralogical Magazine*, 74, 991–998.
- 214 Kampf, A. R., Mills, S. J., Housley, R. M., Rumsey, M. S., and Spratt, J. (2012a) Lead–tellurium
215 oxysalts from Otto Mountain near Baker, California: VII. Chromschieffelinite,
216 $\text{Pb}_{10}\text{Te}_6\text{O}_{20}(\text{CrO}_4)(\text{H}_2\text{O})_5$, the chromate analogue of schieffelinite. *American Mineralogist*,
217 97, 212–219.
- 218 Kampf, A. R., Mills, S. J., Housley, R. M., and Marty, J. (2012b) Lead–tellurium oxysalts from
219 Otto Mountain near Baker, California: IX. Agaite, $\text{Pb}_3\text{Cu}^{2+}\text{Te}^{6+}\text{O}_5(\text{OH})_2(\text{CO}_3)$, a new
220 mineral with CuO_5 – TeO_6 polyhedral sheets. *American Mineralogist*, 97, xxx–xxx.
- 221 Krivovichev, S. V. and Brown, I. D. (2001) Are the compressive effects of encapsulation an
222 artifact of the bond valence parameters? *Zeitschrift für Kristallographie*, 216, 245–247.
- 223 Mills, S.J., Kampf, A.R., Kolitsch, U., Housley, R.M., and Raudsepp, M. (2010) The crystal
224 chemistry and crystal structure of kuksite, $\text{Pb}_3\text{Zn}_3\text{Te}^{6+}\text{P}_2\text{O}_{14}$, and a note on the crystal
225 structure of yafsoanite, $(\text{Ca,Pb})_3\text{Zn}(\text{TeO}_6)_2$. *American Mineralogist*, 95, 933–938.
- 226 Mills, S.J., Kolitsch, U., Miyawaki, R., Groat, L.A., and Poirier, G. (2009) Joëlbruggerite,
227 $\text{Pb}_3\text{Zn}_3(\text{Sb}^{5+}, \text{Te}^{6+})\text{As}_2\text{O}_{13}(\text{OH}, \text{O})$, the Sb^{5+} analogue of dugganite, from the Black Pine
228 mine, Montana. *American Mineralogist*, 94, 1012–1017.

229 Sheldrick, G. M. (2008) A short history of *SHELX*. Acta Crystallographica, A64, 112–122.

230

FIGURE CAPTIONS

231

232

233 Figure 1. SEM image of fuettererite tablets on the cotype specimen.

234

235 Figure 2. Crystal drawings (clinographic projections) of fuettererite showing prismatic (left) and
236 tabular (right) habits.

237

238 Figure 3. Structures of fuettererite (left) and spangolite (right) viewed down [110] with *c* vertical.
239 Unit cells are shown as dashed lines.

240

241 Figure 4. Detail of layers in fuettererite structure with Pb coordination shown in “ball-and-stick”
242 style..Hydrogen bonds are shown as single black lines.

243

244 Figure 5. Pb coordination in fuettererite. The lopsided distributions of bond lengths are
245 attributable to the localization of the lone-pair electrons. Bond lengths are given in Å.

246

247 Figure 6. Octahedral sheets in the structures of fuettererite (top) and spangolite (bottom), in both
248 cases viewed down *c*.

249

250 Table 1. New minerals described from Otto Mountain.

Mineral	Ideal Formula	Reference
Ottoite	$\text{Pb}_2\text{Te}^{6+}\text{O}_5$	Kampf et al. (2010a)
Housleyite	$\text{Pb}_6\text{Cu}^{2+}\text{Te}^{6+}_4\text{O}_{18}(\text{OH})_2$	Kampf et al. (2010b)
Thorneite	$\text{Pb}_6(\text{Te}^{6+}_2\text{O}_{10})(\text{CO}_3)\text{Cl}_2(\text{H}_2\text{O})$	Kampf et al. (2010c)
Markcooperite	$\text{Pb}_2(\text{UO}_2)\text{Te}^{4+}\text{O}_6$	Kampf et al. (2010d)
Timroseite	$\text{Pb}_2\text{Cu}^{2+}_5(\text{Te}^{6+}\text{O}_6)_2(\text{OH})_2$	Kampf et al. (2010e)
Paratimroseite	$\text{Pb}_2\text{Cu}^{2+}_4(\text{Te}^{6+}\text{O}_6)_2(\text{H}_2\text{O})_2$	Kampf et al. (2010e)
Telluroperite	$\text{Pb}_3\text{Te}^{4+}\text{O}_4\text{Cl}_2$	Kampf et al. (2010f)
Chromschieffelinite	$\text{Pb}_{10}\text{Te}^{6+}_6\text{O}_{20}(\text{CrO}_4)(\text{H}_2\text{O})_5$	Kampf et al. (2012a)
Fuettererite	$\text{Pb}_3\text{Cu}^{2+}_6\text{Te}^{6+}\text{O}_6(\text{OH})_7\text{Cl}_5$	This study
Agaité	$\text{Pb}_3\text{Cu}^{2+}\text{Te}^{6+}\text{O}_5(\text{OH})_2(\text{CO}_3)$	Kampf et al. (2012b)

251

252

253 Table 2. Chemical analytical data for fuettererite.

Constituent	Analysis 1	Analysis 2	Average
PbO	41.4(7)	41.5(7)	41.45
CuO	30.1(2)	30.6(3)	30.35
Al ₂ O ₃	0.29(6)	0.17(6)	0.23
TeO ₃	12.5(3)	13.1(3)	12.80
Cl	12.54(10)	11.62(10)	12.08
H ₂ O	3.42	3.68	3.55
O=Cl	-2.83	-2.62	-2.73
Total	97.42	98.05	97.73

254

255

256 Table 3. X-ray powder diffraction data for fuettererite.

257

I_{obs}	d_{obs}	d_{calc}	I_{calc}	hkl	I_{obs}	d_{obs}	d_{calc}	I_{calc}	hkl
7	14.81(5)	14.8937	11	0 0 3	21	1.8389(6)	1.8395	13	3 1 -10
		7.4468	5	0 0 6	19	1.8022(16)	1.8076	9	1 3 -11
23	7.18(3)	7.1830	8	1 0 1	9	1.7846(6)	1.7874	11	1 2 -19
4	6.912(15)	6.9198	9	0 1 2			1.7405	5	1 3 13
44	6.106(3)	6.0977	32	1 0 4	9	1.7339(13)	1.7350	1	3 0 18
9	5.641(11)	5.6430	7	0 1 5			1.7299	1	0 4 8
10	4.973(9)	4.9646	3	0 0 9			1.7059	10	3 1 14
9	4.427(6)	4.4308	6	0 1 8	16	1.7042(4)	1.7021	3	1 1 -24
10	4.196(4)	4.2018	6	1 1 0			1.6650	2	3 2 -2
47	4.0432(10)	4.0439	36	1 1 -3			1.6605	2	0 4 11
100	3.733(5)	3.7234	100	0 0 12			1.6549	4	0 0 27
27	3.697(5)	3.6594	30	1 1 -6	18	1.6508(10)	1.6513	2	2 3 -4
47	3.650(19)	3.6268	11	0 2 1			1.6359	3	3 1 -16
28	3.4575(14)	3.4599	22	0 2 4			1.6339	2	1 2 -22
29	3.3713(9)	3.3701	27	2 0 5			1.6042	3	0 2 25
23	3.212(3)	3.2073	26	1 1 9			1.6009	9	3 1 17
29	3.171(3)	3.1612	22	0 2 7	40	1.5976(12)	1.5997	2	2 3 8
20	3.0488(12)	3.0488	23	2 0 8			1.5996	2	0 3 21
14	2.976(5)	2.9787	10	0 0 15			1.5881	14	4 1 0
		2.9228	4	0 1 14	44	1.5843(3)	1.5868	15	1 2 23
22	2.7902(14)	2.7867	22	1 1 -12			1.5792	7	1 4 3
53	2.749(5)	2.7455	40	1 2 -1			1.5532	6	1 4 6
10	2.729(2)	2.7301	8	2 1 -2	16	1.5467(14)	1.5397	3	1 1 -27
49	2.6686(7)	2.6709	39	1 2 -4			1.5316	5	3 1 -19
26	2.6275(10)	2.6290	26	1 2 5			1.5126	11	4 1 -9
41	2.5289(15)	2.5261	48	1 2 -7	21	1.5088(5)	1.5018	3	2 3 -13
22	2.511(3)	2.4986	11	0 2 13			1.4614	2	0 2 28
13	2.478(6)	2.4720	2	0 1 17	15	1.4594(3)	1.4608	9	4 1 12
		2.4677	6	1 2 8			1.4433	2	0 5 4
8	2.435(3)	2.4300	11	1 1 -15	12	1.4318(4)	1.4330	2	2 3 -16
		2.4259	5	3 0 0			1.4317	6	1 3 22
12	2.416(5)	2.3994	3	2 0 14			1.4085	3	5 0 8
		2.3943	2	0 3 3			1.4038	2	1 1 -30
5	2.3363(6)	2.3424	6	2 1 10	17	1.4007(6)	1.4014	2	1 4 15
38	2.2772(8)	2.2776	28	1 2 11			1.3997	3	1 3 -23
11	2.2150(12)	2.2154	11	0 2 16			1.3944	4	3 3 -3
		2.1476	7	2 1 13			1.3803	8	1 2 -28
26	2.1372(3)	2.1372	8	1 1 -18			1.3765	5	3 3 -6
		2.1306	6	2 0 17			1.3747	2	4 2 -1
		2.1009	3	2 2 0	35	1.3743(3)	1.3727	2	2 4 -2
		2.0836	5	2 1 -14			1.3671	2	0 3 27
13	2.0834(7)	2.0803	2	2 2 -3			1.3650	4	2 4 4
		2.0164	9	1 3 1			1.3480	3	3 3 9
33	2.0117(4)	2.0103	14	3 1 2			1.3445	3	2 4 7
		1.9863	7	3 1 -4	18	1.3389(2)	1.3381	2	3 1 -25
		1.9751	4	0 2 19			1.3378	4	1 4 18
		1.9689	16	3 1 5			1.3145	2	2 4 10
87	1.9637(2)	1.9597	30	1 2 -16			1.3109	3	3 3 12
12	1.9214(7)	1.9245	11	3 1 -7			1.3085	3	1 3 -26
		1.9039	10	2 0 20			1.3065	2	5 1 1
48	1.8999(3)	1.9003	10	1 2 17	24	1.3047(3)	1.3049	2	5 1 -2
		1.8983	4	3 1 8			1.3036	3	2 0 32
		1.8982	9	1 1 21			1.3027	3	4 2 11
11	1.8623(9)	1.8617	9	0 0 24			1.2982	2	5 1 4

258

259

260 Table 4. Data collection and structure refinement details for fuettererite.

261		
262	Diffractometer	Rigaku R-Axis Rapid II
263	X-ray radiation	MoK α ($\lambda = 0.71075$ Å)
264	Temperature	298(2) K
265	Structural Formula	Pb ₃ Cu ²⁺ ₆ Te ⁶⁺ O ₆ (OH) ₇ Cl ₅
266	Space group	<i>R</i> -3
267	Unit cell dimensions	<i>a</i> = 8.4035(12) Å
268		<i>c</i> = 44.681(4) Å
269	<i>Z</i>	6
270	Volume	2732.6(6) Å ³
271	Density (for above formula)	5.552 g cm ⁻³
272	Absorption coefficient	36.835 mm ⁻¹
273	<i>F</i> (000)	4008
274	Crystal size	50 × 40 × 35 μm
275	θ range	3.34 to 25.02°
276	Index ranges	-10 ≤ <i>h</i> ≤ 9, -10 ≤ <i>k</i> ≤ 10, -52 ≤ <i>l</i> ≤ 52
277	Reflections collected/unique	7475/1074 [<i>R</i> _{int} = 0.086]
278	Reflections with <i>F</i> _o > 4σ <i>F</i>	971
279	Completeness to $\theta = 25.02^\circ$	99.2%
280	Max. and min. transmission	0.3588 and 0.2603
281	Refinement method	Full-matrix least-squares on <i>F</i> ²
282	Parameters refined	93
283	GoF	1.053
284	Final <i>R</i> indices [<i>F</i> _o > 4σ <i>F</i>]	<i>R</i> ₁ = 0.0307, <i>wR</i> ₂ = 0.0629
285	<i>R</i> indices (all data)	<i>R</i> ₁ = 0.0350, <i>wR</i> ₂ = 0.0649
286	Largest diff. peak/hole	+2.23/-1.43 e Å ⁻³
287	<i>Notes:</i> <i>R</i> _{int} = $\Sigma F_o^2 - F_o^2(\text{mean}) /\Sigma[F_o^2]$. GoF = $S = \{\Sigma[w(F_o^2 - F_c^2)^2]/(n-p)\}^{1/2}$. <i>R</i> ₁ = $\Sigma F_o -$	
288	$ F_c /\Sigma F_o $. <i>wR</i> ₂ = $\{\Sigma[w(F_o^2 - F_c^2)^2]/\Sigma[w(F_o^2)^2]\}^{1/2}$. <i>w</i> = $1/[\sigma^2(F_o^2) + (aP)^2 + bP]$ where <i>a</i> is 0.0122,	
289	<i>b</i> is 42.3265 and <i>P</i> is $[2F_c^2 + \text{Max}(F_o^2, 0)]/3$.	
290		

291 Table 5. Fractional coordinates and atomic displacement parameters for fuettererite.

292

293

	x/a	y/b	z/c	U_{eq}	U_{11}	U_{22}	U_{33}	U_{23}	U_{13}	U_{12}	
294	Pb	0.31093(5)	0.08441(5)	0.292530(8)	0.02421(16)	0.0252(3)	0.0258(3)	0.0215(2)	0.00081(14)	-0.00011(15)	0.01269(19)
295	Te	0.0000	0.0000	0.21811(2)	0.0151(2)	0.0156(4)	0.0156(4)	0.0142(5)	0.000	0.000	0.00781(18)
296	Cu1	0.29295(15)	0.87164(15)	0.21204(2)	0.0182(3)	0.0174(6)	0.0177(7)	0.0194(6)	0.0004(4)	-0.0015(4)	0.0087(5)
297	Cu2	0.42162(15)	0.29485(15)	0.21574(2)	0.0185(3)	0.0173(6)	0.0177(6)	0.0203(6)	-0.0004(4)	0.0004(4)	0.0087(5)
298	Cl1	0.3333	0.6667	0.1667	0.0238(13)	0.027(2)	0.027(2)	0.018(3)	0.000	0.000	0.0133(10)
299	Cl2	0.6667	0.3333	0.3333	0.0308(14)	0.036(2)	0.036(2)	0.020(3)	0.000	0.000	0.0181(12)
300	Cl3	0.6667	0.3333	0.25842(8)	0.0217(9)	0.0238(14)	0.0238(14)	0.0175(19)	0.000	0.000	0.0119(7)
301	Cl4	0.3307(4)	0.4253(3)	0.30055(5)	0.0282(6)	0.0279(14)	0.0250(14)	0.0293(13)	-0.0021(10)	-0.0002(10)	0.0113(11)
302	O1	0.0805(8)	0.8642(8)	0.19380(12)	0.0169(14)	0.026(4)	0.017(3)	0.014(3)	-0.003(2)	-0.001(2)	0.016(3)
303	O2	0.8640(9)	0.7773(8)	0.24186(12)	0.0192(14)	0.022(4)	0.026(4)	0.013(3)	0.002(3)	0.003(3)	0.014(3)
304	OH3	0.4826(8)	0.1181(9)	0.19776(13)	0.0195(15)	0.020(4)	0.025(4)	0.012(3)	0.000(3)	-0.001(3)	0.010(3)
305	H3	0.490(12)	0.107(12)	0.1781(6)	0.023						
306	OH4	0.3710(8)	0.4889(8)	0.23097(13)	0.0169(14)	0.017(3)	0.017(3)	0.016(3)	0.000(3)	-0.001(3)	0.007(3)
307	H4	0.361(12)	0.477(12)	0.2509(5)	0.020						
308	OH5	0.0000	0.0000	0.3046(2)	0.027(3)	0.031(4)	0.031(4)	0.019(6)	0.000	0.000	0.016(2)
309	H5	0.0000	0.0000	0.3247(5)	0.033						

310

Note: All sites were assigned full occupancy.

311

312 Table 6. Selected bond lengths (Å) in fuettererite.
313

314	Pb–O2	2.385(5)	Cu1–O1	1.935(6)	Cu2–OH3	1.968(6)		
315	Pb–OH5	2.402(2)	Cu1–OH4	1.981(6)	Cu2–OH4	1.999(6)		
316	Pb–Cl4	2.808(2)	Cu1–OH3	1.984(7)	Cu2–OH3	2.003(6)		
317	Pb–Cl4	3.043(3)	Cu1–OH4	2.009(6)	Cu2–O2	2.071(6)		
318	Pb–Cl3	3.0630(18)	Cu1–O2	2.541(6)	Cu2–O1	2.362(6)		
319	Pb–Cl2	3.2222(5)	Cu1–Cl1	2.7888(11)	Cu2–Cl3	2.705(3)		
320	Pb–Cl4	3.262(3)	<Cu–φ>	2.207	<Cu–φ>	2.185		
321	Pb–Cl4	3.357(2)						
322	<Pb–φ>	2.943	Hydrogen bonding					
323			D–H	d(D–H)	d(H...A)	<DHA	d(D...A)	A
324	Te–O1 (×3)	1.927(6)	OH3–H3	0.89(2)	1.75(3)	172(9)	2.634(8)	O1
325	Te–O2 (×3)	1.948(6)	OH4–H4	0.90(2)	2.25(2)	176(8)	3.144(6)	Cl4
326	<Te–O>	1.938	OH5–H5	0.90(2)	2.737(16)	132.5(4)	3.408(9)	Cl4 (×3)

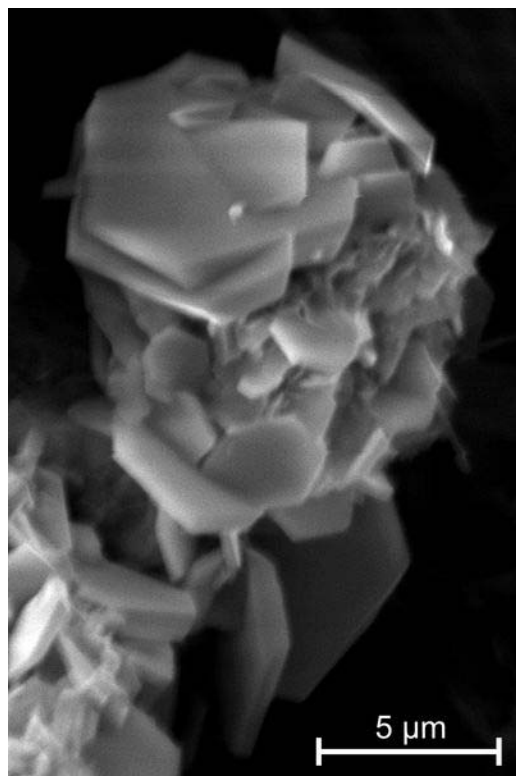
327
328
329

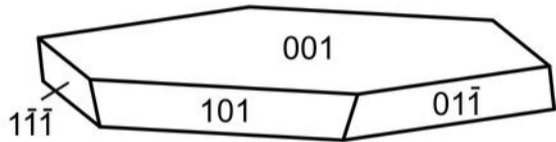
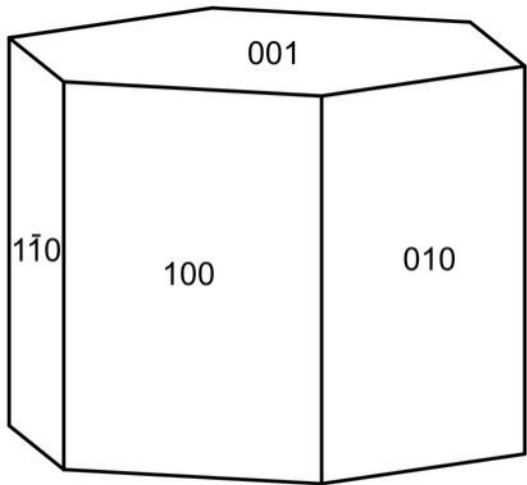
330 Table 7. Bond valence sums for fuettererite. Values are expressed in valence units.
331

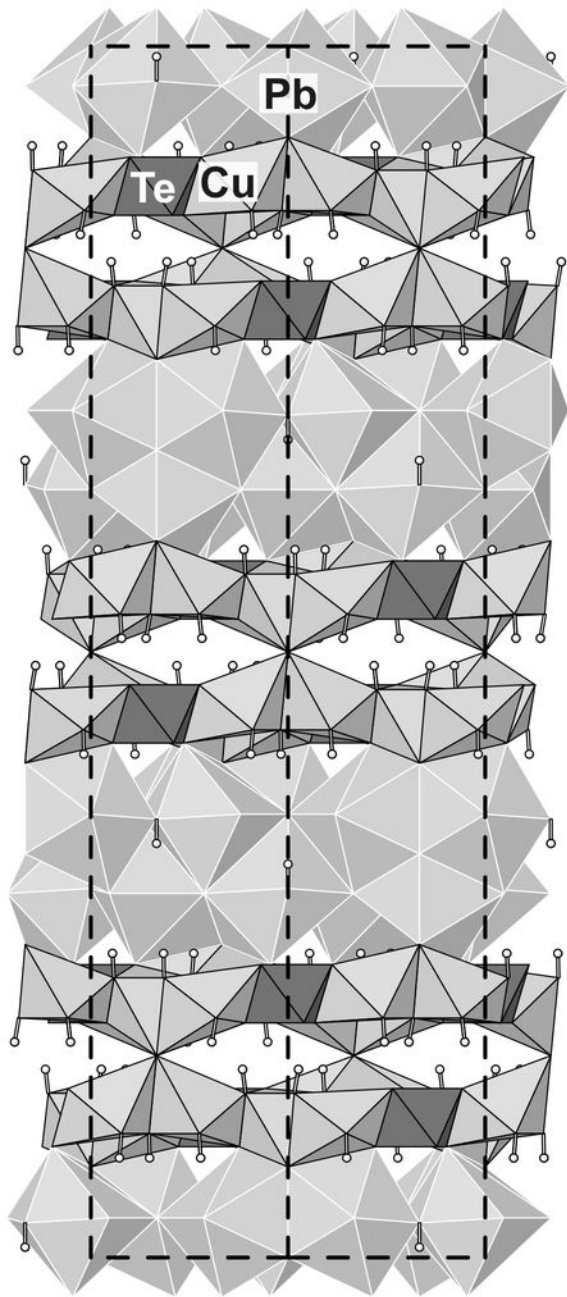
	Cl1	Cl2	Cl3	Cl4	O1	O2	OH3	OH4	OH5	Σ
Pb		0.154 ×6↓	0.237 ×3↓	0.472 0.250 0.138 0.107		0.423			0.408 ×3↓	2.189
Cu1	0.119 ×6↓				0.501	0.097	0.439	0.442 0.410		2.008
Cu2			0.149 ×3↓		0.158	0.347	0.458 0.417	0.421		1.950
Te					0.973 ×3→	0.920 ×3→				5.679
H3					0.205		0.795			1.000
H4				0.195				0.805		1.000
H5				0.075 ×3→					0.775	1.000
Σ	0.714	0.924	1.158	1.237	1.837	1.787	2.109	2.078	1.999	

332 Notes: All values are based upon full occupancies. Multiplicity is indicated by ×→↓. Pb²⁺–O
333 bond strengths from Krivovichev and Brown (2001); Pb²⁺–Cl and Cu²⁺–Cl bond strengths from
334 Brese and O’Keeffe (1991); Te⁶⁺–O and Cu²⁺–O bond strengths from Brown and Altermatt
335 (1985); hydrogen-bond strengths based on H··O and H··Cl bond lengths, also from Brown and
336 Altermatt (1985). .

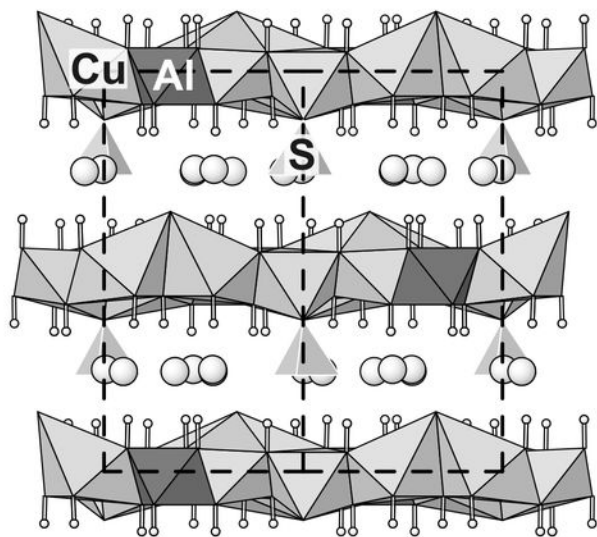
337



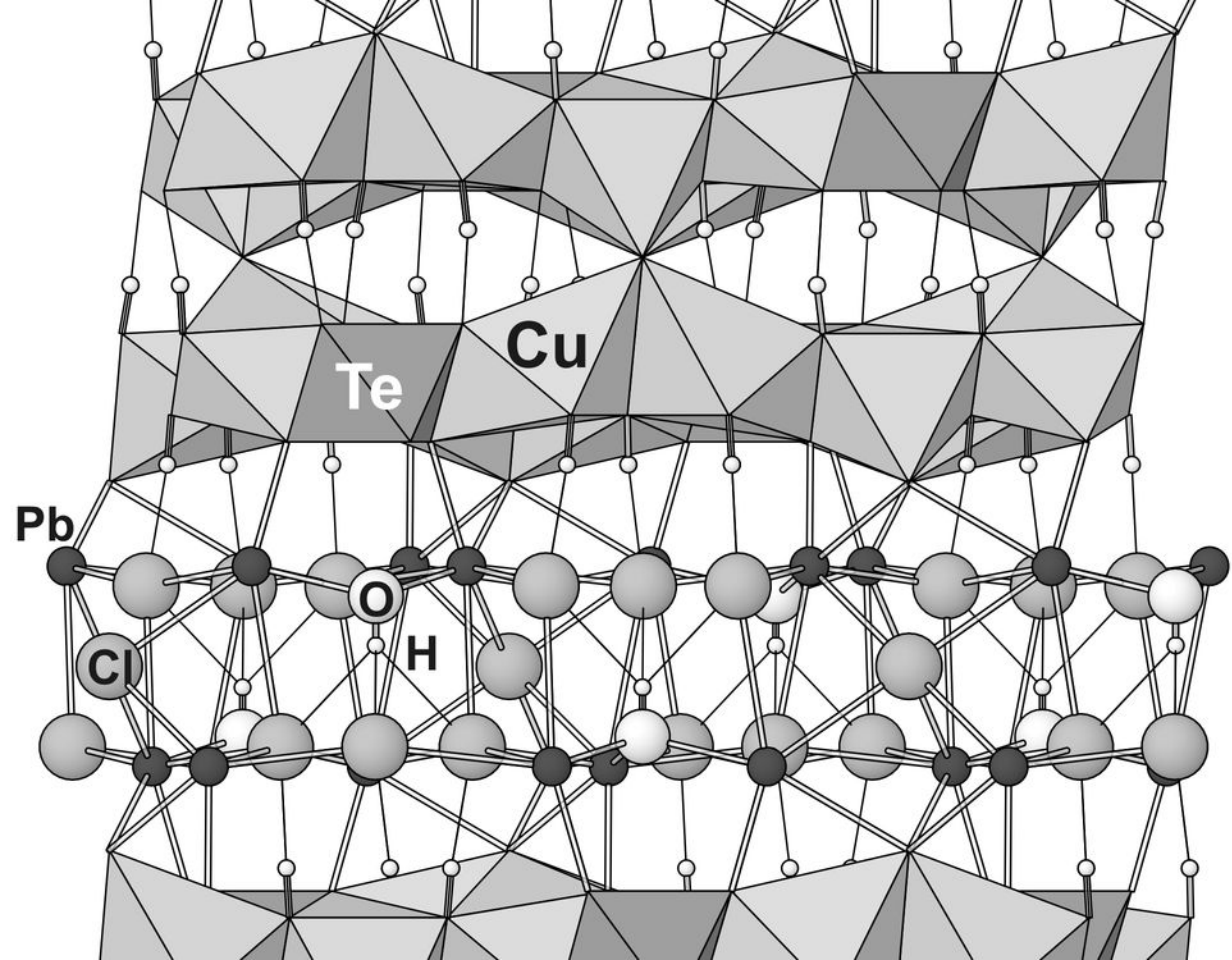


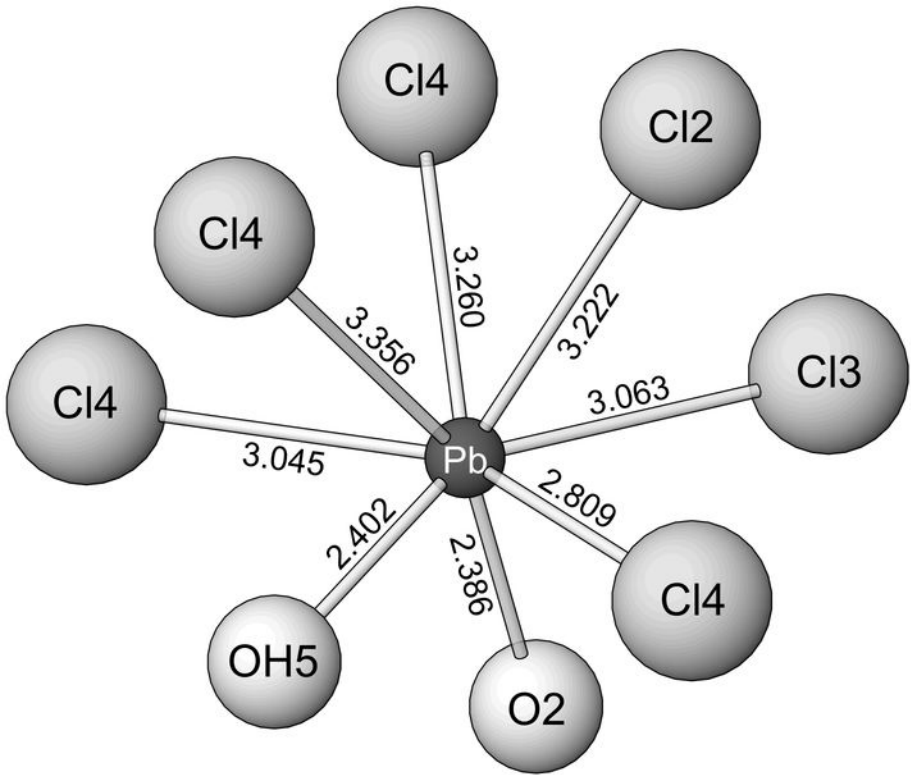


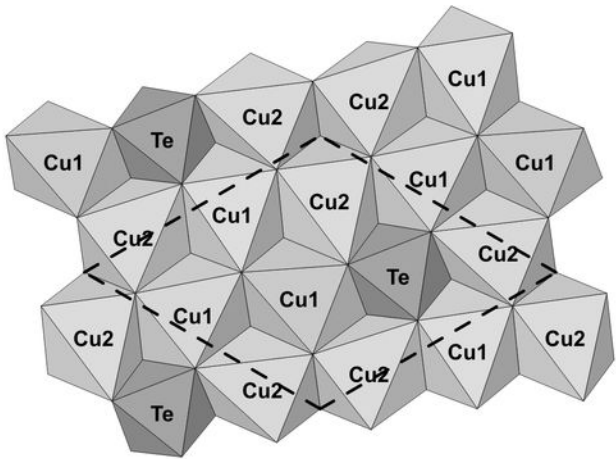
fuettererite



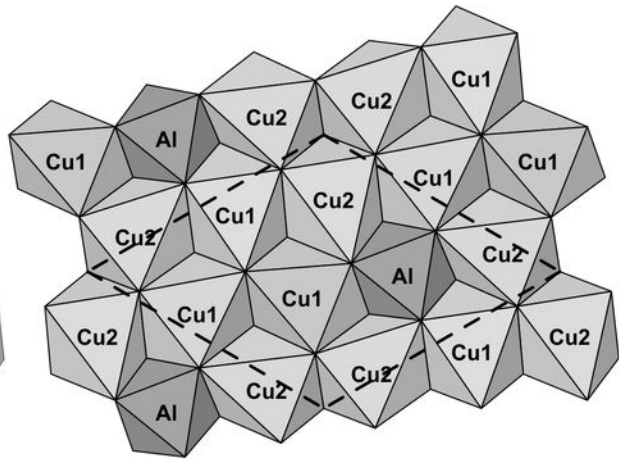
spangolite







fuettererite



spangolite